

perimental assistance.

<sup>1</sup>There has been some confusion in the literature with regard to the names associated with various echo phenomena. Thus, in the present case, polarization echoes {B. P. Smolyakov, N. B. Angert, U. Kh. Kopvillem, and R. Z. Sharipov, *Fiz. Tverd. Tela* **15**, 559 (1973) [*Sov. Phys. Solid State* **15**, 387 (1973)], and references contained therein}, boson echoes and phonon echoes [A. Billman, C. Frénois, J. Joffrin, A. Levelut, and S. Ziolkiewicz, *J. Phys. (Paris)* **34**, 453 (1973), and references contained therein], and electric-field echoes [N. S. Shiren and R. L. Melcher, in *Proceedings of the Ultrasonics Symposium, Milwaukee, Wisconsin, 1974* (Institute of Electrical and Electronics Engineers, New York, 1974), p. 572, and references therein] have all been used. The term "polarization echo" is closest in spirit and meaning to the original spin (magnetization) echo, and we have, therefore, decided to use it henceforth.

<sup>2</sup>Smolyakov *et al.*, Ref. 1.

<sup>3</sup>A. A. Chaban, *Fiz. Tverd. Tela* **15**, 3608 (1973) [*Sov. Phys. Solid State* **15**, 2405 (1974)], and references contained therein.

<sup>4</sup>R. B. Thomson and C. F. Quate, *J. Appl. Phys.* **42**, 907 (1971).

<sup>5</sup>Billman *et al.*, Ref. 1.

<sup>6</sup>P. A. Fedders and E. Y. C. Lu, *Appl. Phys. Lett.* **23**, 502 (1973).

<sup>7</sup>Shiren and Melcher, Ref. 1.

<sup>8</sup>R. R. Haering, *Can J. Phys.* **37**, 1374 (1959).

<sup>9</sup>A. R. Hutson and D. L. White, *J. Appl. Phys.* **33**, 40 (1962).

<sup>10</sup>J. J. Amodei and D. L. Staebler, *RCA Rev.* **33**, 71 (1972).

<sup>11</sup>In the same sample as the experiments reported here only holographic echoes are detected at 10 GHz.

<sup>12</sup>C. Maerfeld and P. Tournois, in *Proceedings of the Ultrasonics Symposium, Milwaukee, Wisconsin, 1974* (Institute of Electrical and Electronics Engineers, New York, 1974), p. 220.

## Study of Superlattice Formation in $2H\text{-NbSe}_2$ and $2H\text{-TaSe}_2$ by Neutron Scattering

D. E. Moncton\*†

*Department of Physics, Massachusetts Institute of Technology, Cambridge, Massachusetts 02139*

and

J. D. Axe\*

*Brookhaven National Laboratory, Upton, New York 11973*

and

F. J. DiSalvo

*Bell Laboratories, Murray Hill, New Jersey 07974*

(Received 27 January 1975)

Neutron-scattering studies of  $2H\text{-NbSe}_2$  and  $2H\text{-TaSe}_2$  reveal the strong Kohn anomalies and incommensurate superlattice characteristic of charge-density-wave instabilities. Whereas the  $\text{NbSe}_2$  superlattice ( $T_0=33.5$  K) remains incommensurate to 5 K,  $\text{TaSe}_2$  ( $T_0=122.3$  K) locks to a commensurate  $3a$  superlattice at 90 K. The temperature dependence of the superlattice wave vector and the lockin behavior are understood using a free energy involving terms third order in atomic displacement. A secondary lattice distortion required by this model is observed.

The unusual changes in the electronic properties<sup>1</sup> of  $2H\text{-NbSe}_2$  near 35 K and  $2H\text{-TaSe}_2$  near 120 K are indicative of a phase transition in which the conduction electrons play an important role. From electron-diffraction studies of  $2H\text{-TaSe}_2$  Wilson, DiSalvo, and Mahajan<sup>2,3</sup> showed that weak superlattice Bragg spots develop at the same temperature as that which characterizes these electronic anomalies. The superlattice appeared to be commensurate with the high-temperature lat-

tice, having  $a'=3a$  and  $c'=c$ . Similar experiments on  $1T\text{-TaSe}_2$  found a high-temperature incommensurate superlattice which becomes commensurate in a strongly first-order transition at 473 K. Since the wave vector characterizing this incommensurate superlattice is changed by doping with Ti, it was concluded that the superlattice results from a charge-density-wave (CDW) instability of the type first suggested by Overhauser.<sup>4</sup> In this Letter we present the results of neu-

tron-scattering experiments which demonstrate that at inception the superlattices of both  $2H$ -TaSe<sub>2</sub> and  $2H$ -NbSe<sub>2</sub> are also slightly incommensurate and furthermore that TaSe<sub>2</sub> undergoes a lockin transition to the  $3a$  superlattice at 90 K.

Our neutron data were obtained on a triple-axis spectrometer at the Brookhaven National Laboratory high-flux beam reactor using mainly high-purity crystals<sup>5</sup> grown by DiSalvo. Unfortunately, the largest are still of relatively small volume for such an experiment (1 to 60 mm<sup>3</sup>). Inelastic scattering employed a variety of incident beam energies, while elastic studies used neutrons in the range 13.0 to 14.5 meV. Tuned pyrolytic-graphite filters eliminated wavelength contamination when necessary.

Our study of the temperature-dependent Bragg intensities shows that superlattice formation occurs in a second-order (or nearly second-order) way in both  $2H$ -NbSe<sub>2</sub> ( $T_0 = 33.5$  K) and  $2H$ -TaSe<sub>2</sub> ( $T_0 = 122.3$  K). At 140 K in TaSe<sub>2</sub> appreciable quasielastic critical scattering<sup>6</sup> with reduced wave vector near  $\bar{a}^*/3$  ( $a^* = 4\pi/\sqrt{3}a$ ) is evident which develops into a system of Bragg superlattice reflections at  $T_0$ . Figure 1 shows the results of high-resolution elastic scans along  $[\zeta 00]$  at various temperatures below  $T_0$  in TaSe<sub>2</sub>. These data provide clear evidence of three novel features of the development of the superlattice.

(1) The wave vector characterizing the superlattice just below  $T_0$  is *not* exactly commensurate with the high-temperature reciprocal lattice, but

is rather  $\vec{q}_\delta = (1 - \delta)\bar{a}^*/3$ , with  $\delta \sim 0.02$ , and temperature dependent.

(2) There exists an apparently first-order phase transformation<sup>7</sup> near 90 K in which  $\delta \rightarrow 0$ , and the superlattice remains commensurate below this temperature.

(3) In the incommensurate regime there exists, in addition to the primary lattice distortion of wave vector  $\vec{q}_\delta$ , a weaker secondary lattice distortion<sup>8</sup> having a wave vector  $\vec{q}_{2\delta} = (1 + 2\delta)\bar{a}^*/3$ . The ultimately successful search for this scattering was motivated by the free-energy considerations to be discussed presently.

In NbSe<sub>2</sub> a similarly incommensurate superlattice is observed below  $T_0$ , yet no lockin transition occurs above 5 K. The sample was too small to observe a  $\vec{q}_{2\delta}$  peak. The temperature dependence of  $\delta$  for both compounds is summarized in Fig. 2(a). Measurements of the Bragg intensity associated with the primary distortion have been made as a function of temperature in both compounds (Fig. 3). Although second-order behavior is apparent, we caution that it is often hard to detect a small first-order discontinuity.

Presumably the microscopic basis for the understanding of these observations involves detailed consideration of electronic charge-density instabilities and their coupling to the lattice. However, a very simple phenomenological theory based upon a Landau-like free-energy expansion provides a clear semiquantitative understanding of the behavior of the incommensurate phases

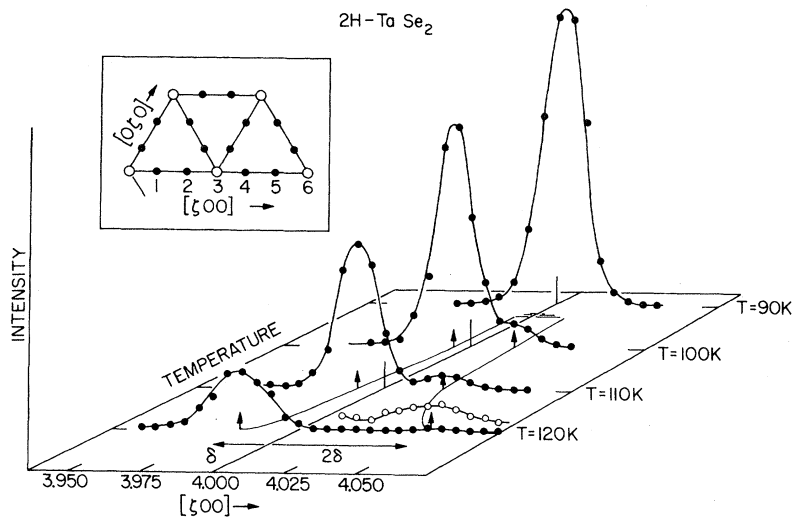


FIG. 1. Elastic scans along  $[\zeta 00]$  showing the incommensurate primary peak at  $\zeta = (4 - \delta)a^*/3$  and a secondary peak at  $\zeta = (4 + 2\delta)a^*/3$ . Open circles indicate multiplication by ten. The inset shows the reciprocal hexagonal superlattice. Open circles are Bragg points of the high-temperature structure; solid circles are the primary superlattice Bragg points of the commensurate superlattice.

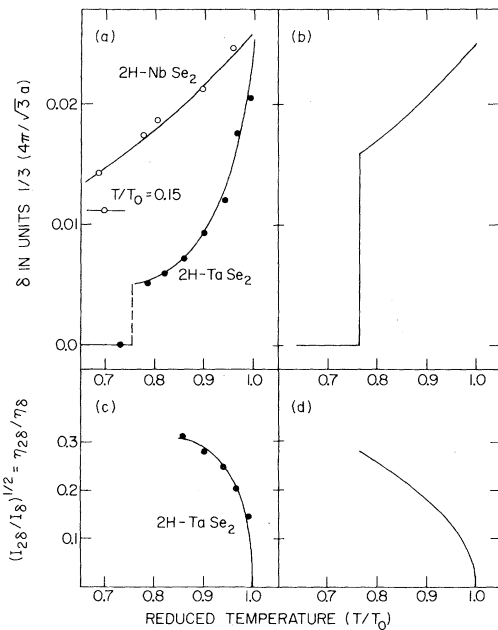


FIG. 2. Temperature dependence of  $\delta$  and  $\eta_{2\delta}/\eta_{\delta}$  as measured, (a) and (c), and as predicted, (b) and (d), by the model described in text.  $B^2/C = 0.87$  ( $9\delta_0^2$ ) for the model curves shown.

discussed above. The expansion is in powers of the order parameters, which we take as the amplitudes of plane-wave distortions with well-defined symmetry properties (normal modes). We find the essential terms in the free energy of the incommensurate state to be

$$F_{\text{inc}} = A(\vec{q}_{\delta}, T)\eta_{\delta}^2 + A(\vec{q}_{2\delta}, T)\eta_{2\delta}^2 - B\eta_{\delta}^2\eta_{2\delta} + \frac{1}{4}C\eta_{\delta}^4, \quad (1)$$

while for the commensurate state

$$F_{\text{com}} = A(\vec{q}_c, T)\eta_c^2 - \frac{1}{3}B\eta_c^3 + \frac{1}{4}C\eta_c^4, \quad (2)$$

where  $\eta_{\delta}$ ,  $\eta_{2\delta}$ , and  $\eta_c$  are the real amplitudes of distortions at wave vectors  $\vec{q}_{\delta}$ ,  $\vec{q}_{2\delta}$ , and  $\vec{q}_c = \vec{a}^*/3$ , respectively. The coefficients  $B$  and  $C$  are assumed constant whereas  $A(\vec{q}, T) = \alpha(T - T_0) + |\vec{q} - \vec{q}_0|^2$ . This is the simplest form of  $A(\vec{q}, T)$  which will lead to a lattice susceptibility diverging at  $T = T_0$  for  $\vec{q} = \vec{q}_0 = (1 - \delta_0)\vec{a}^*/3$ , where  $\delta_0$  is a temperature-independent constant. Terms of the type  $\eta_{\delta}^2\eta_{2\delta}$ , coupling pairs of order parameters, are required by translational invariance. For simplicity, we keep only terms coupling order parameters having wave vectors along the same  $\langle \xi 00 \rangle$  direction.

The temperature-dependent behaviors of  $\eta_c$ ,  $\eta_{\delta}$ ,

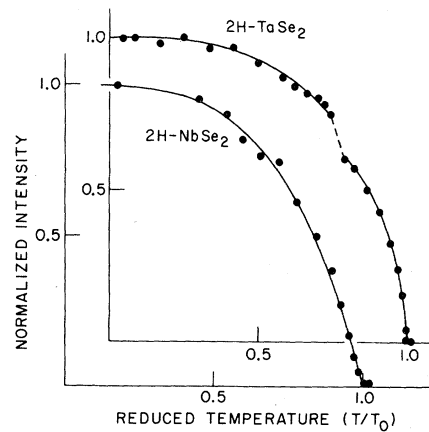


FIG. 3. Normalized intensity of the primary superlattice Bragg peaks versus temperature. The break in the  $\text{TaSe}_2$  curve marks the lockin transition.

$\eta_{2\delta}$ , and  $\delta$  are determined by minimizing the free energies with respect to these variables. There are two distinct cases. If  $B^2/C \geq 9\delta_0^2$  a first-order transition occurs at  $T_{\text{com}} \geq T_0$  with a commensurate ( $\vec{q} = \vec{q}_c$ ) superlattice. However, if  $B^2/C < 9\delta_0^2$  a second-order transition to the incommensurate ( $\vec{q} = \vec{q}_0$ ) state occurs at  $T_0$ . The origin of the temperature dependence of  $\delta$  is the coupling term  $-B\eta_{\delta}^2\eta_{2\delta}$  in Eq. (2) which of course ensures a secondary distortion  $\eta_{2\delta}$ . However, the major contribution to the energy of this secondary distortion,  $A(\vec{q}_{2\delta}, T)\eta_{2\delta}^2$ , can be further reduced if  $\delta$  is decreased. For values of  $B^2/C$  sufficiently close to  $9\delta_0^2$ ,  $F_{\text{com}}$  becomes less than  $F_{\text{inc}}$  at some temperature below  $T_0$  and a first-order lockin transition occurs. Figure 2 shows the data and predictions obtained by minimization of Eqs. (1) and (2) for a roughly optimized set of model parameters. The quantity  $\eta_{2\delta}/\eta_{\delta}$  is simply related to the intensities of the  $\vec{q}_{\delta}$  and  $\vec{q}_{2\delta}$  peaks (Fig. 1) by  $\eta_{2\delta}/\eta_{\delta} = (I_{2\delta}/I_{\delta})^{1/2}$ . The value of  $\alpha$  used in  $A(\vec{q}, T)$  which is necessary to obtain a reasonable lockin temperature differs considerably from the value obtained from the correlation lengths above  $T_0$ . We suspect that a more realistic model including additional  $\vec{q}$  dependence of the coefficients  $A$ ,  $B$ , and  $C$  would rectify this problem.

In order to gain information on the dynamical aspects of these transitions, we have studied most of the phonon branches for the  $[\xi 00]$  and  $[00\xi]$  directions below 12 meV in both materials<sup>5</sup> at 300 K. Figure 4 shows the pronounced Kohn-like anomalies evident in the predominantly longitudinal  $\Sigma_1$  modes at wave vector  $\vec{q}_c = \vec{a}^*/3$ . A similar anomaly has been observed by Wakaba-

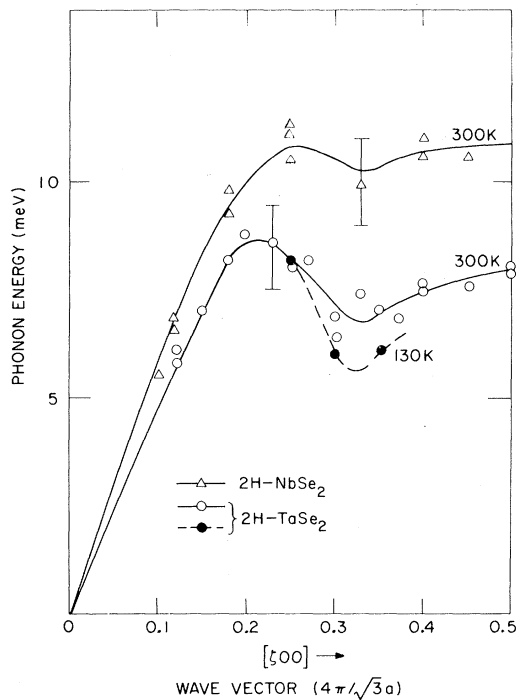


FIG. 4. Dispersion relations for the  $\Sigma_1[\xi 00]$  acoustic phonon branch. Full bar represents the half width of the corresponding neutron group.

yashi<sup>9</sup> in studies of  $\text{NbSe}_2$  (5-at.% Mo). The existence of a Kohn anomaly in a longitudinal mode is a natural consequence of the nesting Fermi surfaces and strong electron-phonon interaction required for a CDW transition. However, the theoretical prediction<sup>10</sup> that the phonon frequency at the critical wave vector goes to zero at  $T_0$  is not borne out for these materials, as is evident from the data of Fig. 4 taken at  $T = 130$  K (just above  $T_0$  in  $\text{TaSe}_2$ ).

Although no soft mode is found, we have shown that the static atomic displacements occurring below  $T_0$  have  $\Sigma_1$  symmetry. Bragg-intensity data taken in the commensurate regime ( $T = 5$  K) of  $\text{TaSe}_2$  were fitted by structure factors calculated using  $\Sigma_1$  phononlike displacements. We find the predominant motion to be that of the Ta atom along  $\vec{q} \parallel [\xi 00]$  (upper limit  $\sim 0.09 \text{ \AA}$ ) which opposes a smaller  $[\xi 00]$  Se atom displacement. Slight movement of the Se atoms along  $[00\xi]$  also occurs. The full details of our study of the low-temperature displacements will be published elsewhere.

The existence of incommensurate superlattices and strong Kohn anomalies can be taken as evi-

dence of the occurrence of CDW instabilities in both  $\text{NbSe}_2$  and  $\text{TaSe}_2$ . We feel it is important, however, to emphasize two aspects of the behavior of these components which seem to fit rather awkwardly within the canonical CDW description. The first of these is the aforementioned absence of a soft phonon mode together with the appearance of quasielastic critical scattering. A relevant microscopic CDW theory must account for this behavior. Secondly, it seems extraordinary that the values of  $\delta$  [Fig. 2(a)] just below  $T_0$  in both materials are essentially identical. Presumably the  $\vec{q}_\delta$  wave vectors are related to their respective Fermi surfaces, yet it would be surprising to find them so nearly equivalent in these two compounds.

It is a pleasure to acknowledge conversations with R. A. Cowley, S. H. Liu, D. Mukamel, R. Pynn, G. Shirane, and J. A. Wilson, which have made an invaluable contribution to our experiments. We thank R. F. Frindt for the loan of a  $\text{NbSe}_2$  crystal, and D. E. M. is grateful to C. G. Shull for his encouragement and support.

\*Work performed under the auspices of the U. S. Atomic Energy Commission.

†Guest scientist at Brookhaven National Laboratory.

<sup>1</sup>H. N. S. Lee, M. Garcia, H. McKinzie, and A. Wold, *J. Solid State Chem.* **1**, 190 (1970).

<sup>2</sup>J. A. Wilson, F. J. DiSalvo, and S. Mahajan, *Phys. Rev. Lett.* **32**, 882 (1974).

<sup>3</sup>J. A. Wilson, F. J. DiSalvo, and S. Mahajan, to be published.

<sup>4</sup>A. W. Overhauser, *Phys. Rev.* **167**, 691 (1968).

<sup>5</sup>A  $\text{NbSe}_2$  crystal kindly lent to us by R. F. Frindt was used in the inelastic measurements. This crystal did not develop a  $\sim 3a$  superlattice. See D. J. Huntley and R. F. Frindt, *Can. J. Phys.* **52**, 861 (1974).

<sup>6</sup>At 123 K in  $\text{TaSe}_2$  the correlation length along  $[\xi 00]$  is three times that along  $[00\xi]$ .

<sup>7</sup>Recent experiments measuring the Young's modulus of  $2H\text{-TaSe}_2$  have shown a sharp anomaly near 90 K. See M. Barmatz, in *Proceedings of the Ultrasonics Symposium, Milwaukee, Wisconsin, 1974* (Institute of Electrical and Electronics Engineers, New York, 1974).

<sup>8</sup>Bragg scattering at wave vector  $\vec{q}_{2\delta}$  can develop simply as a diffraction harmonic from a lattice distortion having only a  $\vec{q}_\delta$  component. However, estimates indicate this effect to be below  $10^{-4}$  times the intensity of the neighboring  $\vec{q}_\delta$  peak. Therefore, the intensity observed at  $\vec{q}_{2\delta}$  requires an actual lattice distortion having wave vector  $\vec{q}_{2\delta}$ .

<sup>9</sup>N. Wakabayashi, H. G. Smith, H. R. Shanks, to be published.

<sup>10</sup>S.-K. Chan and V. Heine, *J. Phys. F: Metal Phys.* **3**, 795 (1973).